Available online at www.sciencedirect.com
SCIENCE DIRECT®
Environmental Research 94 (2004) 67–74
Environmental Research
http://www.elsevier.com/locate/envres

Atmospheric concentrations of the Cl atom, ClO radical, and HO radical in the coastal marine boundary layer

Chang-Tang Chang,[a,*] Tsun-Hsien Liu,[b] and Fu-Tien Jeng[b]

[a] Department of Environmental Engineering, National I-Lan Institute of Technology, No. 1, Sheen-Long Road, I-Lan City 260, Taiwan
[b] Graduate Institute of Environmental Engineering, National Taiwan University, No. 71, Chou-Shan Road, Taipei City 106, Taiwan

Received 7 October 2002; received in revised form 30 June 2003; accepted 16 July 2003

Abstract

Atmospheric concentrations of chlorine atom ($Cl^{\bullet}$), chlorine monoxide radical ($ClO^{\bullet}$), and hydroxyl radical ($HO^{\bullet}$) in the coastal marine boundary layer are estimated in this study. A steady-state approach to their concentrations in equilibrium with other atmospheric chemical species is used. Measurements of atmospheric trace species, HCl, Cl_2, HCHO, H_2O_2, CH_3OOH, CH_4, CO, SO_2, NO, NO_2, and O_3, were performed at four sites in Taiwan during the spring of 1999. The results indicate that the concentrations of the $Cl^{\bullet}$ atom and the $ClO^{\bullet}$ and $HO^{\bullet}$ radicals decrease significantly with cloud cover. The calculated average daytime concentrations of $Cl^{\bullet}$, $ClO^{\bullet}$, and $HO^{\bullet}$ are 3×10^5, 1×10^7, and 6×10^5 molecules/cm^3, respectively. Due to the high reactivity of $Cl^{\bullet}$ with hydrocarbons and its concentration level competitive to that of $HO^{\bullet}$, $Cl^{\bullet}$ should be a significant sink for hydrocarbons in these cases.

Keywords: Chlorine atom; Chlorine monoxide radical; Hydroxyl radical; Atmospheric chemistry modeling; Sea salt aerosol

1. Introduction

The Cl atom converted from chloride originating from sea salt particles plays a significant role in the chemistry of the marine boundary layer (Finlayson-Pitts, 1983; Finlayson-Pitts et al., 1989; Kerminen et al., 1998; Pszenny et al., 1993). Chloride enters the atmosphere in the form of sea spray, and then transfers to the gas phase as HCl in the presence of H_2SO_4 or HNO_3 (Seinfeld and Pandis, 1998):

$$2NaCl_{(s)}+H_2SO_{4(g)}\leftrightarrow Na_2SO_{4(s)}+2HCl,$$
$$NaCl_{(s)}+H_2SO_{4(g)}\leftrightarrow NaHSO_{4(s)}+HCl,$$
$$NaCl_{(s)}+HNO_{3(g)}\leftrightarrow NaNO_{3(s)}+HCl.$$

On the other hand, Cl_2, $ClNO_2$, and NOCl are produced in some polluted areas via the following reactions of sea spray with atmospheric pollutants (Finlayson-Pitts et al., 1989; Seinfeld and Pandis, 1998):

$$N_2O_{5(g)}+NaCl_{(s)}\rightarrow ClNO_{2(g)}+NaNO_{3(s)},$$
$$2NO_{2(g)}+NaCl_{(s)}\rightarrow NOCl_{(g)}+NaNO_{3(s)},$$
$$ClONO_{2(g)}+NaCl_{(s)}\rightarrow Cl2_{(g)}+NaNO_{3(s)}.$$

The gaseous products of the above reactions, HCl, $ClNO_2$, NOCl, and Cl_2, are potential precursors of the chlorine atom through photolysis in the troposphere. Among these products, HCl is the main gas-phase species leading to Cl atom formation, due to the following reaction with the hydroxyl radical (Singh and Kasting, 1988):

$$HCl+HO^{\bullet}\rightarrow Cl^{\bullet}+H_2O.$$

Similar to hydroxyl radicals, chlorine atoms are strong oxidants in the marine boundary layer. Chlorine atoms in polluted areas oxidize volatile organic compounds (VOCs) and lead to the subsequent oxidation reactions. In fact, the reaction rates of chlorine atoms with VOCs in the atmosphere are faster than those of the hydroxyl radical. For example, the reaction rate constant of the chlorine atom with CH_4 in the atmosphere is 1.0×10^{-13} cm^3/molecule/s, while that of hydroxyl is 6.2×10^{-15} cm^3/molecule/s at 25°C (Atkinson et al., 1997). In general, reaction rate constants of chlorine atoms with most VOCs in the gas phase are two orders of magnitude larger than those of the hydroxyl radicals (Atkinson, 1990; Atkinson and Aschman, 1985; Atkinson et al., 1997; Wallington et al., 1988).

*Corresponding author. Fax: 886-39359674.
E-mail address: ctchang@ilantech.edu.tw (C.-T. Chang).

0013-9351/$ - see front matter © 2003 Elsevier Inc. All rights reserved.
doi:10.1016/j.envres.2003.07.008

The atmospheric concentrations of $Cl^{\bullet}$ reported by several investigators essentially fall within the range of 10^3–10^6 molecules/cm^3 (Finlayson-Pitts, 1983; Hewitt et al., 1996; Pszenny et al., 1993). For example, Singh and Kasting (1988) calculated the vertical profile (0–10 km) of the $Cl^{\bullet}$ average concentration to be ca. 10^3 molecules/cm^3 at the marine troposphere by using a one-dimensional photochemical model with detailed chlorine–hydrocarbon photochemistry in the marine troposphere. Pszenny et al. (1993) computed the steady-state concentrations of gas-phase chlorine species other than HCl by using a standard chemistry mechanism with $HCl + HO^{\bullet}$ as the primary $Cl^{\bullet}$ source. According to their results, the noon concentrations of $Cl^{\bullet}$ vary from 10^3 to 10^5 molecules/cm^3. Jobson et al. (1994), based on the reactions of $Cl^{\bullet}$ with several hydrocarbons, estimated the averaged $Cl^{\bullet}$ concentration to be in the range of 3.9×10^3–7.7×10^6 molecules/cm^3 in April at Alert, Northwest Territories, England. These investigations illustrate that the concentration level of $Cl^{\bullet}$ may be significant in the marine troposphere. However, the importance of $Cl^{\bullet}$ in predicting the magnitude of $HO^{\bullet}$ and $ClO^{\bullet}$ radicals is still not clear.

In this study, a photochemistry mechanism based on Cantrell et al. (1996) and Singh and Kasting (1988) is proposed to calculate the $Cl^{\bullet}$ atmospheric concentration. The equations are simplified because some of the reactions do not occur in the lower troposphere. Furthermore, H_2O_2, CH_3O_2H, and HCHO, in addition to HCl and Cl_2, were sampled and analyzed to enhance the estimation of $Cl^{\bullet}$, $HO^{\bullet}$, and $ClO^{\bullet}$ concentrations.

2. Materials and methods

A chemistry model consisting of many important atmospheric chemical species was proposed in this study. Field experiments were conducted in four sites to monitor the concentrations of many species in the atmosphere, including $Cl^{\bullet}$, $ClO^{\bullet}$, and $HO^{\bullet}$.

2.1. Chemistry

A steady-state assumption for reactive radicals was applied in this study to estimate their atmospheric concentrations. Because the transient species ($Cl^{\bullet}$, $ClO^{\bullet}$, and $HO^{\bullet}$) are very reactive compared to other atmospheric chemical species, it is reasonable to assume that they exhibit steady-state concentrations at a given instant in the troposphere (as illustrated by Pszenny et al., 1993). If the concentrations of all trace gases and the physical parameters that control these radicals are measured, then it is feasible to calculate their concentrations. This approach is similar to that of Cantrell et al. (1996) for predicting peroxy radicals.

We assumed that photo-dissociation of chlorinated hydrocarbons did not occur in this study because the short UVC wave of solar radiation does not easily reach the lower troposphere. Some atmospheric species, such as $O^{\bullet}$, $ClONO_2$, ClONO, NOCl, and HOCl, were neglected because their typical concentration levels in marine boundary layers are usually too low to affect other of species interest. The radical $ClOO^{\bullet}$ is mainly produced by the reaction of $Cl^{\bullet}$ with O_2, dissociating back to $Cl^{\bullet}$ and O_2 much faster than it forms. Therefore, this reaction was also neglected in this study. Three key radicals ($Cl^{\bullet}$, $ClO^{\bullet}$, and $HO^{\bullet}$) and two related radicals ($HO_2^{\bullet}$ and $CH_3O_2^{\bullet}$) were considered. A set of equations for these radicals was established to represent their chemical production and loss due to atmospheric photochemical reactions. In the steady state, their concentration time dependencies (dC/dt) were set to zero compared to other atmospheric species. These equations were solved simultaneously by a numerical method to obtain the equilibrium concentrations of these radicals in the atmosphere. All atmospheric reactions considered in this study are summarized in Table 1. Cl-related reactions were adopted from Singh and Kasting (1988). Kinetics data were obtained from Atkinson et al. (1997) and DeMore et al. (1992).

2.2. Field observations

The four sites, Wanli, Kaohsiung, Hengchun, and Chaochou, are designated as Sites A–D (Fig. 1). A is located in northern Taiwan and faces the East China Sea. Site B, a major metropolitan city surrounded by industrial areas, is the most polluted site of the four. Site C was selected for its low pollution level as the background site. These three sites (A–C) are near the ocean. Site D is more inland, with its shortest distance to the ocean being about 30 km.

During the four seasons at four sites, separate air samples were taken for analyses of the following species: HCl, Cl_2, CH_4, HCHO, H_2O_2, and CH_3O_2H. The concentrations of these species are required for the determination of the key radicals as shown in Table 1; e.g., HCHO is involved in reactions 6, 13, 23, 26, and 35. Furthermore, $CH_3O_2^{\bullet}$ and $HO_2^{\bullet}$ radicals were also calculated simultaneously with $HO^{\bullet}$, $Cl^{\bullet}$, and $ClO^{\bullet}$ because they are needed to describe the production and loss of key radicals. Futhermore, the measured HCl and Cl_2 concentrations, (shown in Fig. 4) were used to validate the predicted results of HCl and Cl_2 concentrations with modeling. Aerosol samples were also taken with glass fiber filters to measure atmospheric Na^+ and Cl^- concentrations in the aerosol phase. The experiment periods and sample durations for each site are tabulated in Table 2.

Samples were taken about 12 m above the ground at four sites. Different air samples were taken for different

Table 1
Atmospheric chemical reactions

	Reaction	Rate coefficient (cm^3/molecule/s)	Ref.
(1)	$O_3 + h\nu \rightarrow O^{\bullet} \cdot (^1D) + O_2$	j_{O_3} [c]	a
(2a)	$O^{\bullet}(^1D) + H_2O \rightarrow 2\,HO^{\bullet}$	2.2×10^{-10}	a
(2b)	$O^{\bullet}(^1D) + O_2 \rightarrow O^{\bullet}(^3P) + O_2$	$3.2 \times 10^{-11} e^{(67/T)}$	a
(2c)	$O^{\bullet}(^1D) + N_2 \rightarrow O^{\bullet}(^3P) + N_2$	$1.8 \times 10^{-11} e^{(107/T)}$	a
(3)	$HO^{\bullet} + CH_4(+O_2) \rightarrow H_2O + CH_3O_2^{\bullet}$	$2.3 \times 10^{-12} e^{(-1765/T)}$	a
(4)	$HO^{\bullet} + CO(+O_2) \rightarrow HO_2^{\bullet} + CO_2$	$1.3 \times 10^{-13}\,(1 + 0.6P/\mathrm{bar}) \times (300/T)^{1.0}$	a
(5)	$HO^{\bullet} + O_3 \rightarrow HO_2^{\bullet} + O_2$	$1.9 \times 10^{-12} e^{(-1000/T)}$	a
(6)	$HO^{\bullet} + HCHO(+O_2) \rightarrow H_2O + HO_2^{\bullet} + CO$	$8.6 \times 10^{-12} e^{(20/T)}$	a
(7)	$HO^{\bullet} + H_2O_2 \rightarrow H_2O + HO_2^{\bullet}$	$2.9 \times 10^{-12} e^{(-160/T)}$	a
(8)	$HO^{\bullet} + CH_3O_2H \rightarrow H_2O + CH_3O_2^{\bullet}$	$1.9 \times 10^{-12} e^{(190/T)}$	a
(9)	$HO^{\bullet} + H_2(+O_2) \rightarrow H_2O + HO_2^{\bullet}$	$7.7 \times 10^{-12} e^{(-2100/T)}$	a
(10)	$HO^{\bullet} + SO_2(+O_2) \rightarrow SO_3 + HO_2^{\bullet}$	2×10^{-12}	a
(11)	$HO^{\bullet} + NO_2 + M \rightarrow HNO_3 + M$	$6.7 \times 10^{-11} (T/300)^{-0.6}$	a
(12)	$HO^{\bullet} + HO_2^{\bullet} \rightarrow H_2O + O_2$	$4.8 \times 10^{-11} e^{(250/T)}$	a
(13a)	$2CH_3O_2^{\bullet} \rightarrow CH_3OH + HCHO + O_2$	$k_{13a} + k_{13b} + k_{13c} = 1.1 \times 10^{-13} e^{(365/T)}$	a
(13b)	$2CH_3O_2^{\bullet} \rightarrow 2CH_3O^{\bullet} + O_2$		a
(13c)	$2CH_3O_2^{\bullet} \rightarrow CH_3OOCH_3 + HCHO + O_2$		a
(14)	$CH_3O_2^{\bullet} + NO \rightarrow CH_3O^{\bullet} + NO_2$	$4.2 \times 10^{-12} e^{(180/T)}$	a
(15)	$HO_2^{\bullet} + CH_3O_2^{\bullet} \rightarrow O_2 + CH_3O_2H$	$3.8 \times 10^{-13} e^{(780/T)}$	a
(16)	$HO_2^{\bullet} + HO_2^{\bullet} \rightarrow H_2O_2 + O_2$	$2.2 \times 10^{-13} e^{(600/T)}$	a
(17)	$HO_2^{\bullet} + NO \rightarrow HO^{\bullet} + NO_2$	$3.7 \times 10^{-12} e^{(240/T)}$	a
(18)	$HO_2^{\bullet} + O_3 \rightarrow HO^{\bullet} + 2O_2$	$1.4 \times 10^{-14} e^{(-600/T)}$	a
(19)	$ClO^{\bullet} + NO \rightarrow Cl^{\bullet} + NO_2$	$6.2 \times 1^{-12} e^{(294/T)}$	a
(20)	$Cl^{\bullet} + CH_4(+O_2) \rightarrow HCl + CH_3O_2^{\bullet}$	$9.6 \times 10^{-12} e^{(-1350/T)}$	a
(21)	$Cl^{\bullet} + O_3 \rightarrow ClO^{\bullet} + O_2$	$2.9 \times 10^{-11} e^{(-260/T)}$	a
(22)	$Cl^{\bullet} + H_2O_2 \rightarrow HCl + HO_2$	$1.1 \times 10^{-11} e^{(-980/T)}$	a
(23)	$Cl^{\bullet} + CH_3O_2H \rightarrow HCHO + HO^{\bullet} + HCl$	5.9×10^{-11}	a
(24)	$Cl^{\bullet} + H_2(+O_2) \rightarrow HCl + HO_2^{\bullet}$	$3.7 \times 10^{-11} e^{(-2300/T)}$	a
(25a)	$Cl^{\bullet} + HO_2^{\bullet} \rightarrow HCl + O_2$	$1.8 \times 10^{-11} e^{(170/T)}$	a
(25b)	$Cl^{\bullet} + HO_2^{\bullet} \rightarrow ClO^{\bullet} + HO^{\bullet}$	$4.1 \times 10^{-11} e^{(-450/T)}$	a
(26)	$Cl^{\bullet} + HCHO(+O_2) \rightarrow HCl + HO_2^{\bullet} + CO$	$8.4 \times 10^{-11} e^{(-34/T)}$	a
(27)	$HO^{\bullet} + ClO^{\bullet} \rightarrow HO_2^{\bullet} + Cl^{\bullet}$	$1.1 \times 10^{-11} e^{(120/T)}$	a
(28)	$HO^{\bullet} + HCl \rightarrow H_2O + Cl^{\bullet}$	$2.4 \times 10^{-12} e^{(-330/T)}$	a
(29a)	$HO_2^{\bullet} + ClO^{\bullet} \rightarrow HOCl + O_2$	$k_{29a} + k_{29b} = 4.6 \times 10^{-13} e^{(-710/T)}$	a
(29b)	$HO_2^{\bullet} + ClO^{\bullet} \rightarrow HCl + O_3$		a
(30)	$HO^{\bullet} + Cl_2 \rightarrow HOCl + Cl^{\bullet}$	$1.4 \times 10^{-12} e^{(-900/T)}$	a
(31)	$Cl^{\bullet} + CO + M \rightarrow ClCO + M$	$1.3 \times 10^{-33} (T/300)^{-3.8} [N_2]$	a
(32)	$Cl^{\bullet} + NO + M \rightarrow ClNO + M$	$2.3 \times 10^{-12} (T/300)^{-1.6}$	b
(33a)	$Cl^{\bullet} + NO_2 + M \rightarrow ClONO + M$	1.6×10^{-11}	b
(33b)	$Cl^{\bullet} + NO_2 + M \rightarrow ClNO_2 + M$	3.6×10^{-12}	b
(34)	$ClO^{\bullet} + NO_2 + M \rightarrow ClONO_2 + M$	2.4×10^{-12}	b
(35)	$HCHO + h\nu \rightarrow 2HO_2^{\bullet} + CO$	j_{HCHO} [c]	a
(36)	$H_2O_2 + h\nu \rightarrow 2HO^{\bullet}$	$j_{H_2O_2}$ [c]	a
(37)	$CH_3O_2H + h\nu \rightarrow CH_3O^{\bullet} + HO^{\bullet}$	$j_{CH_3O_2H}$ [c]	a
(38)	$Cl_2 + h\nu \rightarrow 2Cl^{\bullet}$	j_{Cl_2} [c]	a

[a] Atkinson et al. (1997).
[b] DeMore et al. (1992).
[c] The Photolysis rate constant was estimated by Atkinson et al. (1997).

species. Samples for HCl analysis were collected using an SKC pump with a Supelco ORBO-53 adsorber. Cl_2 was also retained by the SKC pump with a silver membrane filter, extracted and stabilized into chloride by the $Na_2S_2O_3$ solution, and analyzed by an ion chromatograph. Both HCl and Cl_2 were sampled in 3-h intervals during the day (06:00–18:00) and 6-h intervals at night (18:00–06:00). Formaldehyde was adsorbed in the 2,4-dinitrophenylhydrazine-HCl-CH_3CN solution during the same intervals and analyzed by high-performance liquid chromatography, as suggested by Lee and Zhou (1993). Samples for H_2O_2 and CH_3OOH were collected in the midpoint of 3- or 6-h experiment intervals and analyzed by an automated fluorometric method (Lazrus et al., 1985). CH_4 was measured with an autoanalyzer. At each site was also a monitoring station operated by the Taiwan Environment Protection Agency (TWEPA), which provided the hourly atmospheric CO, SO_2, NO, NO_2, and O_3 concentration data for this study. The manufacturers and detection limits of

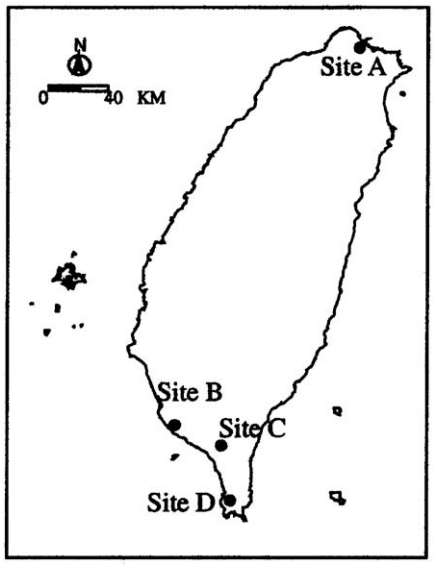

Fig. 1. Experiment field sites. Site A, 121°41′E, 25°11′N; Site B, 120°19′E, 22°11′N; Site C, 120°32′E, 22°33′N; Site D, 120°43′E, 22°01′N.

Table 2
Sampling period and total hours at each experimental site

Site no.	Site name	Period (date and time)	Total hours
A	Wanli	1/29 at 18:00–1/31 at 18:00	24
B	Kaoshuang	2/3 at 18:00–2/6 at 18:00	72
C	Henchun	2/7 at 00:00–2/10 at 12:00	84
D	Chaucho	4/29 at 06:00–4/30 at 18:00	36

Table 3
Detection limit and manufacturer of analyzers used in this study

Species	Detection limit	Manufacturer and model of analyzer
Cl_2	50 ppt	Dionex DX-120
HCl	100 ppt	Dionex DX-120
CH_4	10 ppb	Signal Model 3000
H_2O_2	30 ppt	Turner Designs TD-700
CH_3O_2H	50 ppt	Turner Designs TD-700
HCHO	270 ppt	Waters HPLC 486 Tunable Absorbance Detector
Cl^-	0.016 mg/L[a]	Dionex DX-120
Na^+	0.008 mg/L[a]	Perkin–Elmer AA Model 500

[a] Measured in the aqueous phase.

the above analyzers are listed in Table 3. Teflon and quartz filters were used to collect the aerosol, the collected mass of which can be measured with an electric balance method under constant humidity and temperature. To guarantee the reproducibility of the results with statistical accuracy, the variation within 3% of the concentration of every species at each site in each season was maintained for qualitative evaluation of the data sampling. In addition, the measured species concentrations were determined using the average of at least three samples.

3. Results

3.1. Field observations

Meteorological parameters, temperature, pressure, and cloud cover were measured during the experiment periods at these four sites. For Site A, the weather was cloudy in the beginning (100% cloud cover) and became clearer later in the experiment period. The cloud cover at Sites B and C was less than 50% during the experiment periods, except on February 10 at Site C, when it was 100%. The cloud cover at Site D was 100% during the entire experiment period.

Monitoring data obtained from TWEPA for NO_x and O_3 are illustrated in Figs. 2a and b, respectively. As expected, polluted Site B exhibited the highest NO_x concentration levels, whereas the background Site C had negligible NO_x concentrations. For O_3 concentration, a diurnal pattern was noted at all four sites, specifically at Site B, with O_3 concentrations ranging from 4 to 67 ppb. The high NO_x emissions from Site B react with O_3 at night, resulting in insignificant O_3 levels at that time. O_3 at Site C remains at almost the same concentration (40 ppb) because of the negligible NO_x concentration used to consume O_3.

Time-series plots of Cl_2 and HCl at all sites are shown in Fig. 3. The observed atmospheric concentrations of HCl and Cl_2 at all samples ranged from BD (below the detection level) to 3900 ppt and BD to 580 ppt,

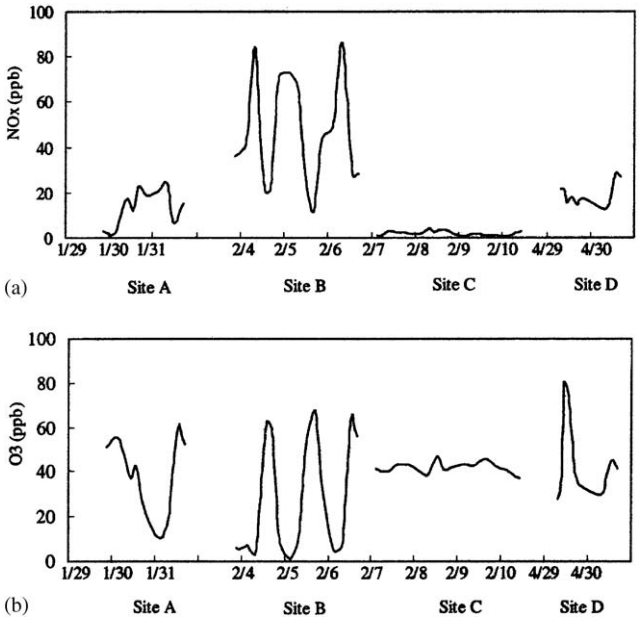

Fig. 2. Concentration profiles of (a) NO_x and (b) O_3 at the four sites.

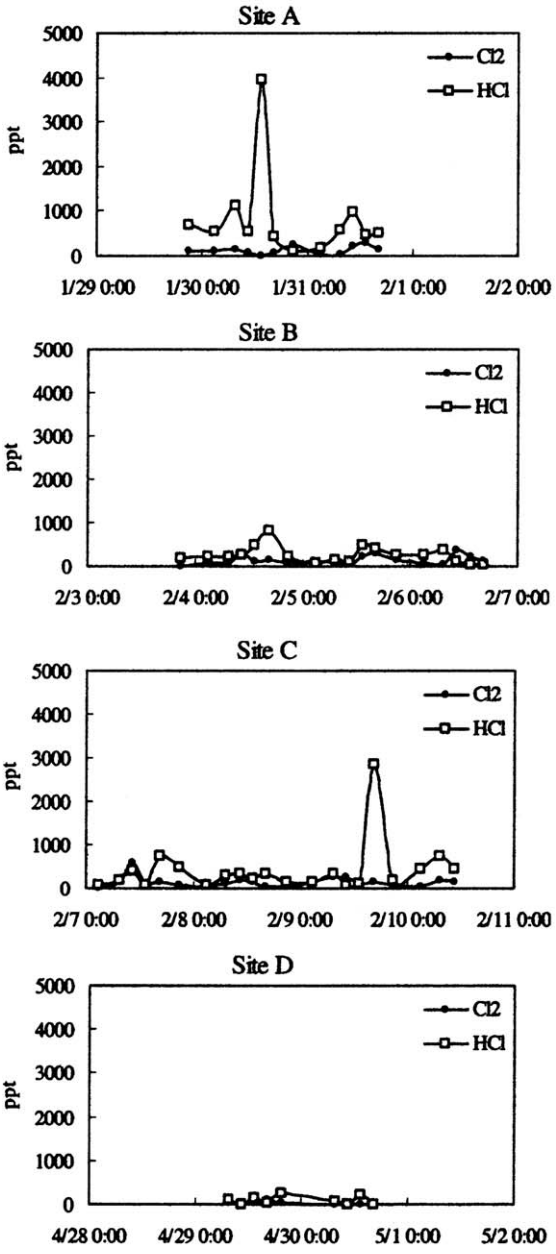

Fig. 3. Measured concentration profiles of HCl and Cl_2.

respectively. In Fig. 3, the Cl_2 and HCl concentrations at Sites A–C were comparable while those at Site D were almost negligible. A larger deficit of aerosol chloride was also observed at Site D, as shown in the Cl/Na ratio column in Fig. 3. The Cl/Na ratio ranged from 0.2 to 1.2, which was significantly less than that at the other sites. This is due to the distance from the ocean. Without any other significant sources, gaseous HCl and Cl_2 are mainly produced from chloride in sea aerosol in the presence of H_2SO_4, HNO_3, NO_x, and other atmospheric pollutants. The chloride concentration and gaseous HCl/Cl_2 in Site D were less than the values in the other sites; as the air mass containing sea aerosols must travel a longer distance to Site D, the chloride is removed by deposition and reactions with pollutants.

The diurnal pattern of HCl/Cl_2 was not significant in this study; most of the daytime concentration levels were greater than those measured at night. The trends of the Cl_2 and HCl concentration profiles, however, were similar at Sites A–C for most of the experiment. Pszenny et al. (1993) deduced in his study that the diurnal trend of Cl_2 is opposite to that of HCl. Our results are somewhat different from his findings.

3.2. Estimated radical concentrations

In this study, the measured and predicted concentrations of Cl_2 were compared to validate the simulation model. As shown in Fig. 4 the peaks of the measured Cl_2 concentrations were almost the same as those of the predicted Cl_2. The estimated performances of the model were accurate, although the measured values were slightly greater than the predicted values.

3.2.1. Chlorine atom

Time-series plots of estimated atmospheric $Cl^{\bullet}$ concentrations are shown in Fig. 5. The calculations of these radicals are based on the measurements of the chemical species shown in Fig. 3 and the data obtained from TWEPA. The pressure data shown in Fig. 3 were

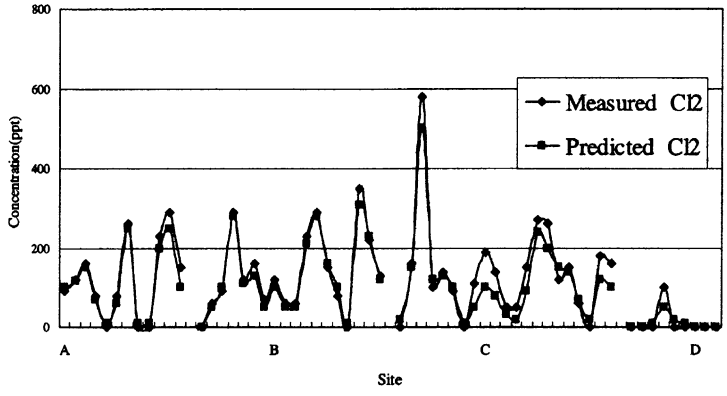

Fig. 4. Comparison between the measured and predicted concentrations of Cl_2.

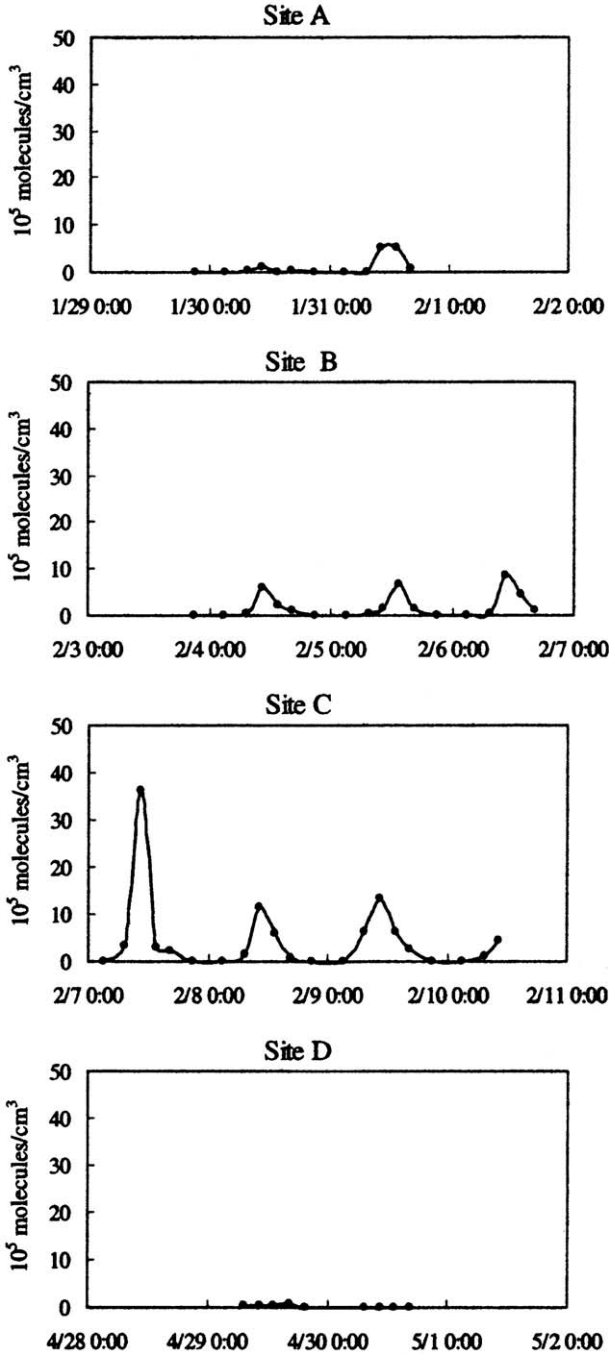

Fig. 5. Time series of calculated Cl• concentrations.

used to convert the data units. The Cl• concentration at Site D was insignificant, possibly due to two factors: (1) 100% cloud cover and (2) negligible concentrations of HCl/Cl_2, the most likely source of Cl• in the atmosphere. Conversely, the high HCl concentration levels with less than 50% cloud cover (as in Site C) certainly produce more Cl•. The Site C results further show a typical diurnal pattern with a daytime (06:00–18:00) average of about 7×10^5 molecules/cm^3. The Cl• concentrations at Site B were less than those at Site C because many pollutants (NO_x, CO, and VOCs) generated at Site B eventually consume Cl• in the atmosphere, as in reactions 26 and 31–33 in Table 1.

3.2.2. Chlorine monoxide radical

The profiles for the ClO• concentrations were similar to those of Cl• radial, except that the concentrations at Site B were insignificant (Fig. 6). The ClO• radical is produced from Cl• (Reactions 21 and 25b in Table 1) and consumed by reactions with NO_x (Reactions 19 and 34 in Table 1). Since Site B was near several industrial

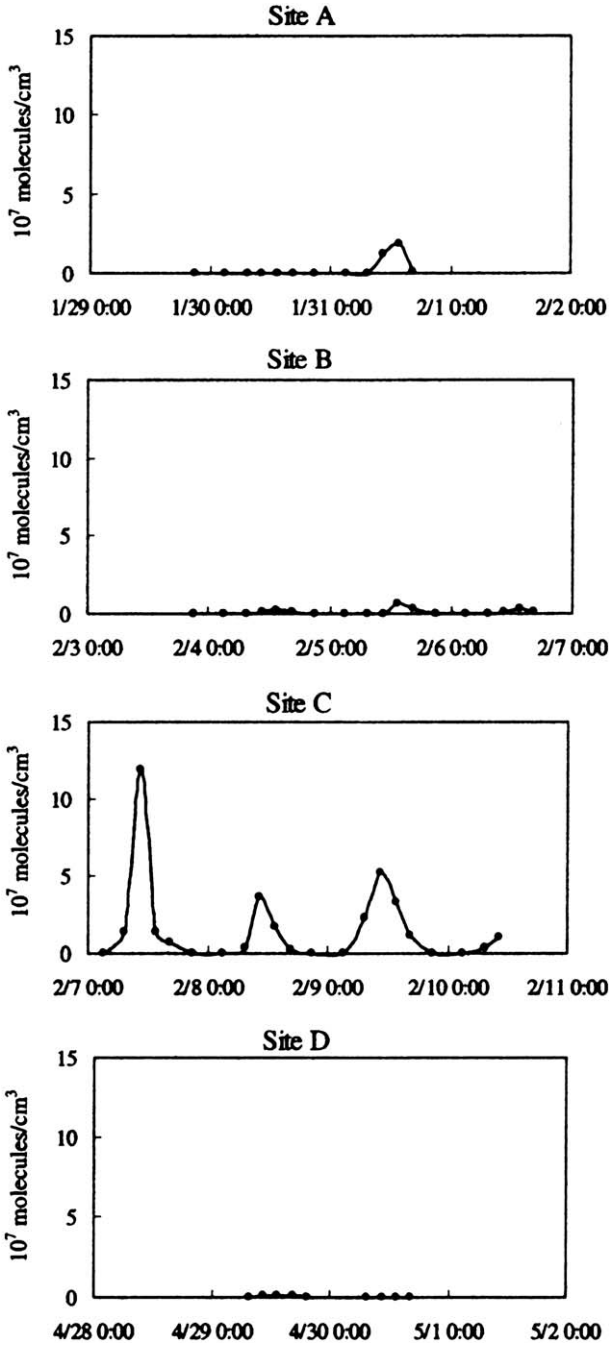

Fig. 6. Time series of calculated ClO• concentrations.

parks, the atmosphere was polluted with NO_x, resulting in insignificant $ClO^{\bullet}$ concentrations. Again, concentrations at Site C show a diurnal pattern with an average peak concentration of about 8×10^7 molecules/cm^3 and average daytime level of 2.5×10^7 molecules/cm^3.

3.2.3. Hydroxyl radical

The $HO^{\bullet}$ concentration profiles in the atmosphere for all sites are shown in Fig. 7. The daytime maximum (noon) concentrations ranged from 1×10^5 to 4×10^6 molecules/cm^3. The average daytime concentration for all sites is 6×10^5 molecules/cm^3, which is the same level as that reported by others (Graedel, 1979; Mather et al., 1997; Singh and Kasting, 1988). The $HO^{\bullet}$ concentration levels at Site C were the greatest of the four sites, with those at Site D being the lowest. Different cloud conditions at the four sites may have caused different $HO^{\bullet}$ concentration levels. More solar radiation (less cloud cover) leads to more $HO^{\bullet}$ production (Reaction 36 in Table 1). This is exemplified at Site A, where $HO^{\bullet}$ concentrations were low initially (when it was cloudy) and then reached a much higher level later concurrent with increasing sunny weather. The low concentration level at Site D (100% cloud cover) also supports this elucidation.

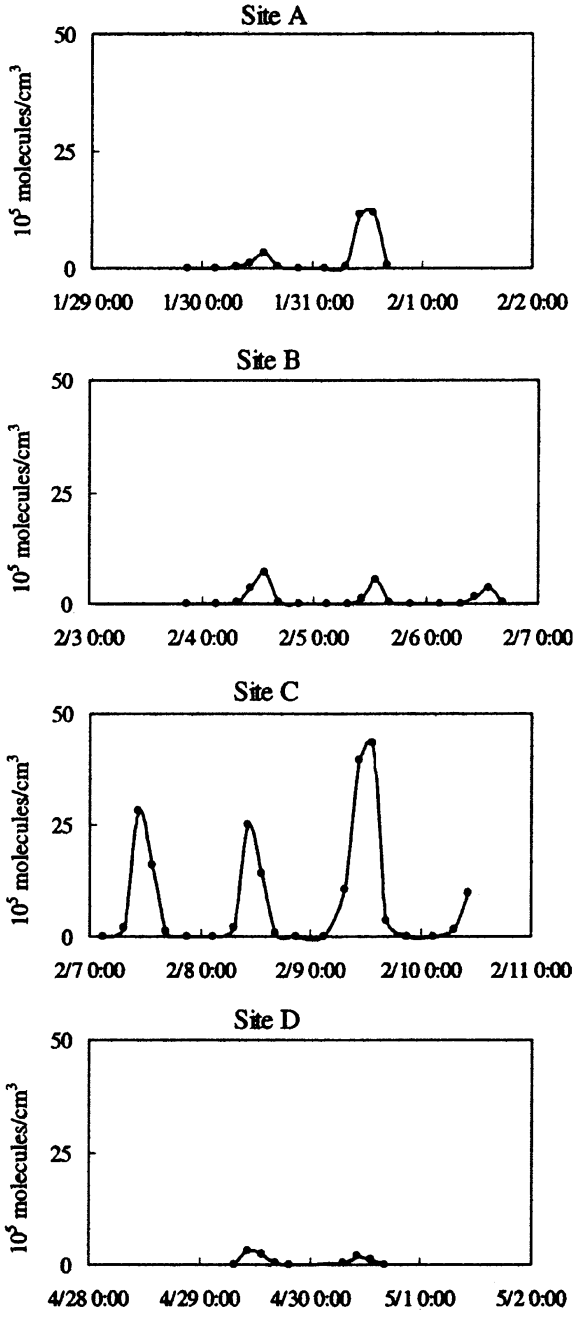

Fig. 7. Time series of calculated $HO^{\bullet}$ concentrations.

4. Discussion and conclusions

The most important of these finding is that concentration levels of the $Cl^{\bullet}$ atom, and the $ClO^{\bullet}$ and $HO^{\bullet}$ radicals decrease significantly with cloud cover. Since most atmospheric chemistry mechanisms applied in air quality modeling do not consider $Cl^{\bullet}$ and other related chlorine species, an assessment of the influence of $Cl^{\bullet}$ on $HO^{\bullet}$ was evaluated in this study. If chlorine photochemistry is not considered in calculating the concentration of $HO^{\bullet}$, i.e., if reactions 19–34 and reaction 38 in Table 1 are ignored in calculating the concentration of $HO^{\bullet}$, the results (not shown) are lower than those for which $Cl^{\bullet}$ is considered, as low as 20% in some cases. Both $Cl^{\bullet}$ and $HO^{\bullet}$ radicals are consumed by their reactions with hydrocarbons, and as discussed earlier, the $Cl^{\bullet}$ reaction with hydrocarbons is faster than that of the $HO^{\bullet}$ radical. This results in a lesser amount of $HO^{\bullet}$ being "consumed" in the presence of $Cl^{\bullet}$. In addition, the oxidized hydrocarbon $R^{\bullet}$ radicals may lead to the further production of $HO^{\bullet}$ in subsequent reactions with O_2. Thus, lower $HO^{\bullet}$ concentrations would be expected if chlorine photochemistry were not considered. However, chlorine photochemistry had no effect at Site D due to the overcast conditions. There is nearly no difference between the two estimated concentrations of $HO^{\bullet}$. Overcast conditions prevent the production of both $Cl^{\bullet}$ and $HO^{\bullet}$, as shown in Fig. 8.

Measurement data at four sites show that Site B is much more polluted with respect to NO_x and VOCs than the others, resulting in more ozone consumption at night. For example, the atmospheric concentration level of ozone at Site B was only 4 ppb at night, which was significantly lower than the background concentration of 40 ppb observed at Site C. The estimated average daytime concentration levels of $Cl^{\bullet}$, $ClO^{\bullet}$, and $HO^{\bullet}$ were 3×10^5, 1×10^7, and 6×10^5 molecules/cm^3, respectively, at Site B. The $Cl^{\bullet}$ and $HO^{\bullet}$ concentration levels are dominated by solar radiation; this is also true for $ClO^{\bullet}$, though atmospheric pollutants also play a significant role. Distance from the ocean may be an

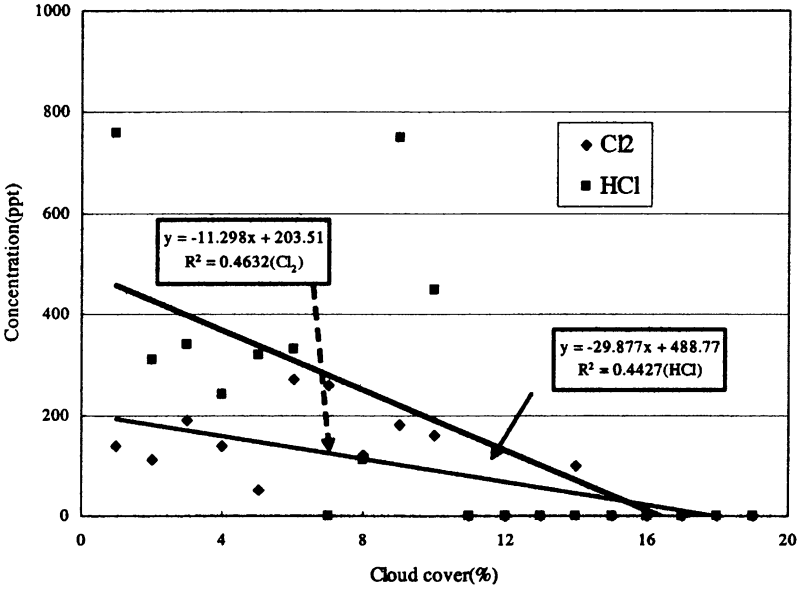

Fig. 8. Relationship between chloride concentration and cloud cover.

important factor in $Cl^{\bullet}$ and $ClO^{\bullet}$ concentrations, since a larger chlorine deficit was observed in sea aerosols at the inland site.

Since the $Cl^{\bullet}$ and $HO^{\bullet}$ concentration levels were in the same order of magnitude and $Cl^{\bullet}$ is more reactive than $HO^{\bullet}$ with VOCs, the Cl species radical definitely plays an important role in the marine boundary layer.

References

Atkinson, R., 1990. Gas-phase tropospheric chemistry of organic compounds: a review. Atmos. Environ. 24A, 1–41.

Atkinson, R., Aschman, S.M., 1985. Kinetics of the gas phase reaction of Cl atoms with a series of organics at 298 ± 2 K and atmospheric pressure. Int. J. Chem. Kinet. 17, 33–241.

Atkinson, R., Baulch, D.L., Cox, R.A., Hampson Jr., R.F., Kerr, J.A., Rossi, M.J., Troe, J., 1997. Evaluated kinetic, photochemical and heterogeneous data for atmospheric chemistry. J. Phys. Chem. Ref. Data 21, 521–1011.

Cantrell, C.A., Shetter, R.E., Gilpin, T.M., Calvert, J.G., Eisele, F.L., Tanner, D.J., 1996. Peroxy radical concentrations measured and calculated from trace gas measurements in the Mauna Loa observatory photochemistry experiment 2. J. Geophys. Res.—Atmos. 101 (D9), 14653–14664.

DeMore, W.B., Sander, S.P., Golden, D.M., Hampson, R.F., Kurylo, M.J., Howard, C.J., Ravishankara, A.R., Kolb, C.E., Molina, M.J., 1992. Chemical kinetics and photochemical data for use in stratospheric modeling. In: "JPL Publication 92-20", Jet Propulsion Laboratory, California Institute of Technology, Pasadena, CA, USA.

Finlayson-Pitts, B.J., 1983. Reaction of NO_2 with nacl and atmospheric implication for NOC1 formation. Nature 306, 676–677.

Finlayson-Pitts, B.J., Ezell, M.J., Pitts Jr., J.N., 1989. Formation of chemically active chlorine compounds by reactions of atmospheric NaCl particles with gaseous N_2O_5 and $ClONO_2$. Nature 337, 241–244.

Graedel, T.E., 1979. The kinetic photochemistry of the marine atmosphere. J. Geophys. Res. 84, 273–286.

Hewitt, A.D., Brahan, K.M., Boone, F.D., Hewitt, S.A., 1996. Kinetics and mechanism of the Cl + CO reaction in air. Int. J. Chem. Kinet. 28, 763–771.

Jobson, B.T., Niki, H., Yokouchi, Y., Bottenheim, J., Hopper, F., Leaitch, R., 1994. Measurements of C2–C6 hydrocarbons during the polar sunrise 1992 experiments: evidence for Cl atom and Br atom chemistry. J. Geophys. Res.—Atmos. 99, 25355–25368.

Kerminen, V.-M., Teinilä, K., Hillamo, R., Pakkanen, T., 1998. Substitution of chloride in sea-salt particles by inorganic and organic anions. J. Aerosol Sci. 29, 929–942.

Lazrus, A.L., Kok, G.L., Gitlin, S.N., Lind, J.A., 1985. Automated fluorometric method for hydrogen peroxide in atmospheric precipitation. Anal. Chem. 57, 917–922.

Lee, Y.N., Zhou, X., 1993. Method for determination of some soluble atmospheric carbonyl compounds. Environ. Sci. Technol. 27, 749–756.

Mather, J.H., Stevens, P.S., Brune, W.H., 1997. OH and HO_2 measurements using laser-induced fluorescence. J. Geophys. Res.—Atmos. 102, 6427–6436.

Pszenny, A.A.P., Keene, W.C., Jacob, D.J., Fan, S., Maben, J.R., Zetwo, M.P., Springer-Young, M., Galloway, J.N., 1993. Evidence of inorganic chlorine gases other than hydrogen chloride in marine surface air. Geophys. Res. Lett. 20, 699–702.

Seinfeld, J.H., Pandis, S.N., 1998. From air pollution to climate change. In: Seinfeld, J.H., Pandis, S.N. (Eds.), Atmospheric Chemistry and Physics. Wiley-Interscience, New York.

Singh, H.B., Kasting, J.F., 1988. Chlorine–hydrocarbon photochemistry in the marine troposphere and lower stratosphere. J. Atmos. Chem. 7, 261–285.

Wallington, T.J., Skewers, L M., Siegel, W.O., 1988. Kinetics of gas phase reaction of chlorine atoms with a series of alkenes, alkynes and aromatic species at 295 K. J. Photochem. Photobiol. 45, 167–175.